Behavior of Concrete Filled Aluminum Square and Rectangular Hollow Section Columns under Axial Loads: Experimental and Analytical Study

Mazin A. Al-Mazini **Aqeel H. Chkhewier**
College of Engineering, Basrah University, Basrah, Iraq
Almazini_engineer@yahoo.com Aqeelcivil@yahoo.com

Abstract

The research presents experimental results square and rectangular aluminum tube columns filled with concrete and analyze these results by finite element method. The studied parameters included the depth to wall thickness ratio (D/t), slenderness ratio of the aluminum tube and concrete core compressive strength. The experimental work included testing of twenty five composite concrete-filled aluminum columns subject to axial load. The depth to thickness ratio of the square and rectangle hollow columns ranged from 25 to 62.5. The column length to depth ratio ranged from 3 to 10. Different filled concrete strengths of 25, 40 and 60 MPa were used. The column strengths, load-axial shortening relationship, load-lateral deformation relationship and failure modes of columns were presented and discussed. The experimental results showed that; the ultimate load of hollow and filled columns increases with the decrease of the depth/ thickness ratio. The compressive strength exhibited very clear effect on the strength of columns filled with concrete. Three-dimensional nonlinear finite element analysis has been used to conduct the analytical investigation; ANSYS (version 12.0) computer program was used in this study. This model was validated by comparison of the experimental and numerical results of ultimate load, load-deformation curves and their corresponding modes of collapse. The analytical results from modeling in ANASYS program exhibited a good agreement with experimental results.

Keywords: concrete filled aluminum column, Confined columns, Composite columns

الخلاصة

هذا البحث يعرض نتائج عملية لاعمدة المربعة والمستطيلة الشكل من الالمنيوم المملؤة بالخرسانة وتحليل هذه النتائج بطريقة العناصر المحددة. المتغيرات التي تمت دراستها هي نسبة العرض/ سمك الجدار ونسبة النحافة لأعمدة ألمنيوم المجوفة وكذلك تأثير مقاومة الانضغاط للقلب الخرساني. يتضمن الجزء العملي فحص خمسة وعشرون نموذج من اعمدة الالمنيوم المملوءة بالخرسانة والمجوفه والمعرضة الى حمل ضغط محوري. نسبة العرض الى سمك الانبوب المربع والمستطيل كانت تتراوح ما بين 25 الى 62.5. ونسبة طول الانبوب الى قطره كانت تتراوح مابين 3 الى 10. استخدمت قيم مختلفة لمقاومة الخرسانة المائة 25، 40 و 60 MPa لبحث عن تأثير تغير المقاومة للخرسانة. تم قياس مقاومة الاعمدة ورسم علاقات مابين التقلص المحوري والحمل ومابين التشوه الجانبي والحمل وكذلك شكل الفشل للنماذج التي فحصت. بينت النتائج العملية ان،الحمل الاقصى للاعمدة المجوفة والمركبة من الالمنيوم والكونكريت تقل بزيادة نسبة العرض /السمك (D/t) و مقاومة العمود المركبة تزداد بزيادة مقاومة الخرسانة. وقد استخدم التحليل اللاخطي للعناصر المحددة بأستخدام البرنامج (ANSYS version 12) لمعرفة السلوك الأنشائي للاعمدة المركبة من الالمنيوم والكونكريت التي تم فحصها عمليا. بينت النتائج ان هنالك توافق جيد عند المقارنة مابين النتائج العملية والنظرية.

الكلمات المفتاحية : عمود المنيوم مملوء بالخرسانة ، اعمدة مطوقة ، اعمدة مركبة

1. Introduction

Aluminum has been used as a structural material because of its light weight material, resistant of the corrosion and ease of product. Modulus of elasticity of the aluminum alloy is less than the modulus of the carbon steel by one third, therefore the ultimate strength, yield stress and stiffness of the carbon steel is more than those of aluminum. So that the overall capacity of the carbon steel column is greater than that of the column aluminum. The aluminum column has been filled with concrete to increase the load carrying capacity of the column. Thereby the stiffness and strength of the column will increase.

Many researchers conducted many experimental investigations on the behavior and strength of circular , square and rectangular steel tubes filled with concrete [Uy (1998, 2001) ; Aboutaba and Machado ,1999 ; Elremaily and Azizinamini , 2002 ; Han ,2002 ; Sakino *et.al.*, 2004 ; Wang *et.al.,* 2004 ; Liu ,2005 ; Tao *et.al.*, 2007].

(Young and Ellobody ,2006) performed tests for stainless steel hollow columns filled with concrete, and it was found that the strength and behavior of these columns are affected by local buckling of both stainless and steel steel tubes. This was attributed to the fact, that as local buckling of steel and stainless steel has occurred, the tube confinement to the core concrete vanished.

(Zhu and Young ,2006) tested many aluminum hollow columns. It was mainly observed that the local buckling, overall buckling or interaction of local and overall buckling of columns was included in the failure modes..

Experimental investigation of aluminum circular hollow section filled with concrete (CHS) stub column was conducted by(Zhou and Yong ,2009). A series of tests was carried out to investigate the effect of the geometric dimension of the aluminum CHS and concrete strength on the behavior and strength of CHS stub column. It was seen that the stiffness of the columns filled with concrete developed as compared to the hollow aluminum CHS stub columns. It has been also, shown that the ductility of the concrete-filled columns decreases with the increase of the concrete compressive strength, especially for columns having relative slender section.

(Resan ,2014) studied experimentally the behavior of aluminum tubes filled with light weight concrete having circular tube section. It was concluded that aluminum-lightweight concrete columns exhibited high capacity increments as compared to the aluminum columns and it provided sufficient lateral support to the light weight core.

2. Research significance

The aim of this study is to assess the effectiveness of the concrete filled aluminum tube column. The studied parameters included: (a) shape of the aluminum tube (square SHS or rectangle RHS hollow section) (b) different strength of the concrete. The investigation consists of two parts; the first part is to investigate experimentally twenty five concrete-filled aluminum tube column. The second part deals with the analysis of the tested columns theoretically. The finite element method, using the software ANSYS version 12.0, was used to model the concrete-filled aluminum columns. The validity of the used analysis is examined with the results of the experimental work.

3. Experimental Investigation

3.1 Details of test specimens

The tests were carried out on square and rectangular aluminum tubes (SHS and RHS, respectively) filled with concrete that had different compressive strength. The aluminum test specimens were fabricated by extrusion using 6063-T6 heat-treated aluminum alloys. Tests were carried out on twenty five specimens, included fourteen square tubes and eleven rectangle tubes. Details of these tubes are presented in Table (1). The section size of the columns is D x B x t, where D is the overall depth, B is the overall width and t is the plate thickness, as shown in Fig. (1). The specimen designation is labeled according to the shape of aluminum tube. The symbol SHS indicates the square section and RHS represents the rectangular section.

Table 1: Details of the tested specimens

Series	Specimens designation	D mm	B mm	t mm	f'_c MPa	D/t	L/D
S1	SHS1	100	100	1.6	25	62.5	3
	SHS2	100	100	2	25	50	3
	SHS3	100	100	3	25	33.3	3
	SHS4	100	100	4	25	25	3
S2	SHS5	100	100	1.6	----	50	3
	SHS6	100	100	1.6	40	50	3
	SHS7	100	100	1.6	60	50	3
S3	SHS8	100	100	2	----	50	3
	SHS9	100	100	2	----	50	5
	SHS10	100	100	2	25	50	5
	SHS11	100	100	2	----	50	7
	SHS12	100	100	2	25	50	7
	SHS13	100	100	2	----	50	10
	SHS14	100	100	2	25	50	10
R1	RHS1	50	100	1.6	25	62.5	3
	RHS2	50	100	2	25	50	3
	RHS3	50	100	3	25	33.3	3
	RHS4	50	100	4	25	25	3
R2	RHS5	50	100	2	----	50	3
	RHS6	50	100	2	----	50	5
	RHS7	50	100	2	25	50	5
	RHS8	50	100	2	----	50	7
	RHS9	50	100	2	25	50	7
	RHS10	50	100	2	----	50	10
	RHS11	50	100	2	25	50	10

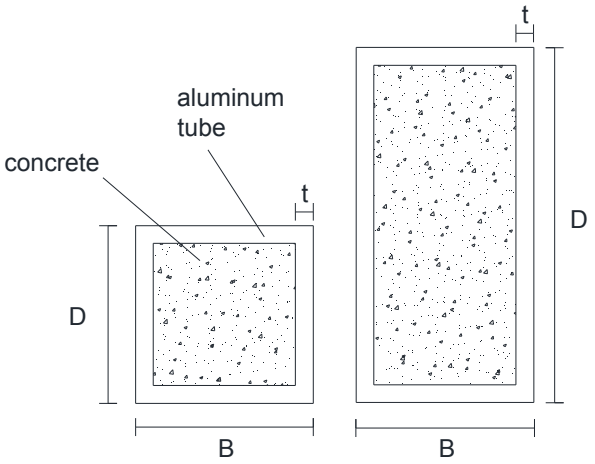

Figure 1: Definition of symbols for concrete-filled aluminum square and rectangular hollow section specimens

2.2. Material properties

1-Concrete

Three concrete mixes with design strength 25, 40 and 60 MPa were made using the locally available materials. The mixes were cast in Construction Materials Lab of Engineering College – Basrah University. Mix design of all compressive strength

grades was carried out according to the British method (British ,1997). The mix proportions are shown in Table (2). Standard concrete cube (150*150*150 mm) specimens were cast to determine the compressive strength.

Table 2: Details of concrete mixes

Quantities of Basic ingredients (Kg/m^3)	Grade of concrete		
	C25	C40	C60
Cement	380	425	500
Fine aggregate	740	722	710
Coarse aggregate	1100	1083	1040
water	195	170	150
Super plasticizer	1.5	4.5	7.5

2. Aluminum alloy tubes

The aluminum coupons cut from the center of the web of untested specimens in the longitudinal direction. The coupons were prepared and tested according to Australian Standard AS 1391(1991) for the tensile strength of materials. The coupon dimensions are 12.5 mm wide and gauge length 50 mm were tested in Construction Materials Lab of Engineering College – Basrah University. Table (3) shows the coupons properties (static 0.2% tensile proof stress ($\sigma_{0.2}$), static ultimate tensile strength (σ_u) and initial Young′s modulus (E_a)).

Table 3: Measured properties of aluminum coupon

No. of coupon	Yield stress, $\sigma_{0.2}$ (MPa)	Ultimate strength σ_u (MPa)	E (GPa)
1	240.2	262.1	66.2
2	250.4	268.5	70.5
3	248.1	269.2	69.4
1	255.6	274.5	71.4
2	260.3	277.2	68.5
3	259.8	289.6	70.1

2.4. Test procedure and instrumentation

The instrumentations were used to detect the structural behaviour of the columns at every stage of loading. To apply compressive axial force, a Torsee′s Universal Testing Machine with capacity 2000 kN at the laboratory of construction materials-University of Basrah was used. Prior to testing, the ends of specimens have been milled flat. The ends of the columns were then capped with plaster to make the application of load on loaded faces of the columns uniformly. The vertical displacement was measured by a dial gauge with accuracy 0.01 mm per division. Dial gage was also setup at the middle of the column to read the lateral displacement. Fig.(2) depicts the test setup. The load on columns was applied monotonically in increments. The maximum load recorded by the testing machine was considered as the ultimate load.

Figure 2: Test setup.

4. Results and Discussion

A summary of experimental results of composite aluminum columns are presented in Table (4).

Table (4): Experimental results of tested columns

Series	Specimens designation	D mm	B mm	t mm	f'_c MPa	D/t	L/D	P_{ult} kN
S1	SHS1	100	100	1.6	25	62.5	3	153
	SHS2	100	100	2	25	50	3	176
	SHS3	100	100	3	25	33.3	3	343
	SHS4	100	100	4	25	25	3	480
S2	SHS5	100	100	1.6	----	50	3	121
	SHS6	100	100	1.6	40	50	3	214
	SHS7	100	100	1.6	60	50	3	321
S3	SHS8	100	100	2	----	50	3	139
	SHS9	100	100	2	----	50	5	107
	SHS10	100	100	2	25	50	5	140
	SHS11	100	100	2	----	50	7	77
	SHS12	100	100	2	25	50	7	92
	SHS13	100	100	2	----	50	10	69
	SHS14	100	100	2	25	50	10	81
R1	RHS1	50	100	1.6	25	62.5	3	70
	RHS2	50	100	2	25	50	3	79
	RHS3	50	100	3	25	33.3	3	150
	RHS4	50	100	4	25	25	3	200
R2	RHS5	50	100	2	----	50	3	64
	RHS6	50	100	2	----	50	5	562
	RHS7	50	100	2	25	50	5	66
	RHS8	50	100	2	----	50	7	49
	RHS9	50	100	2	25	50	7	54
	RHS10	50	100	2	----	50	10	41
	RHS11	50	100	2	25	50	10	45

●P_{ult} is the ultimate load of the concrete filled aluminum column.

4.1. Effect of the depth to wall thickness ratio (D/t)

The effect of D/t ratio on the behavior of the composite aluminum columns was studied. For this purpose, two series (i.e. S1 and R1) were tested. Fig.(3) shows the experimental results of series S1 and R1. Load-axial deformation relations of the columns of S1 group are shown in Fig.(4) and (5).

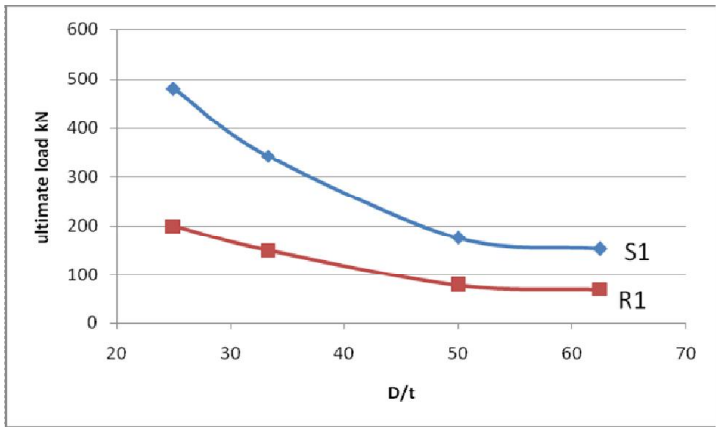

Figure 3: Relationships between ultimate load and D/t

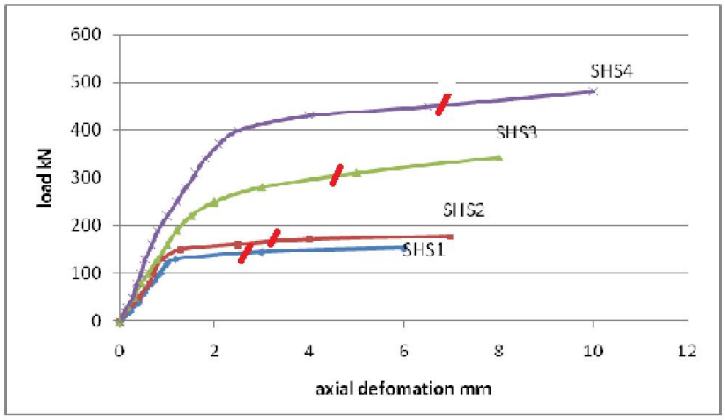

Figure 4: Load versus axial deformation curves the composite columns of series S1

Test results are separated depending on the tube shape; therefore these graphs show the behaviors for the square and rectangular aluminum tube separately. In general, the composite-aluminum columns exhibited various post-yield behaviors depending on the tube wall thickness. Specimens SHS4 and RHS4 (with small D/t) exhibited strain hardening behavior. While specimens with large D/t ratio were classified as elastic perfectly plastic. Specimens SHS3 and RHS3 appeared to be in transition between elastic-plastic and degrading stiffness.

Fig.(6) shows the failure mode of the specimens for S1 and R1 series. All the specimens (square and rectangular sections) failed by wall local buckling of the aluminum tube. Square and rectangular tubes had very similar local buckling. They exhibited clear indications of wall tube bulging. Local buckling occurred equally on every side for the square section. While in the rectangular section, local buckling extended more for the board face compared to that for the narrow face. Overall, the higher local buckling and apparent distortions of specimens have large D/t ratios as compared to the small D/t ratios of the specimens.

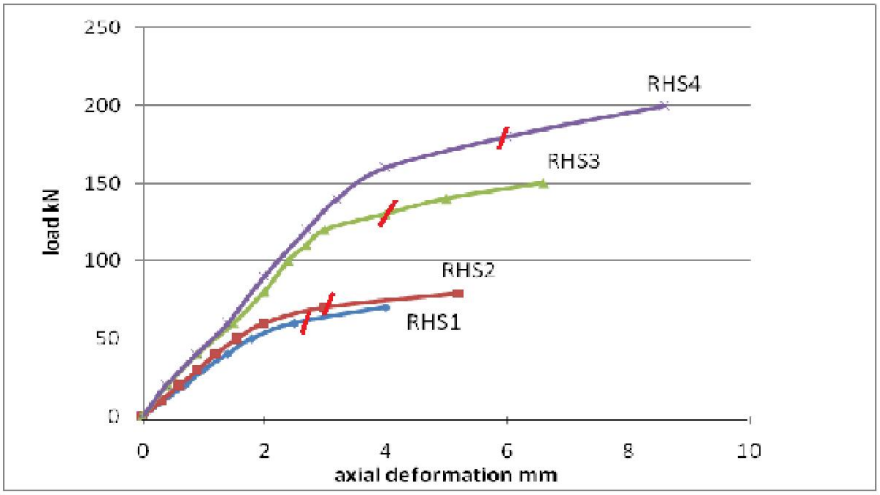

Figure 5: Load versus axial deformation curves for the composite columns of series R1

The approximate values of the observed local buckling of the tube was recorded and marked on the curves in Figs.(4) and (5). It is shown that the local buckling for any specimen occur after yielding the concrete filled aluminum tube. That means that the aluminum tube wall buckles when the axial deformation of the composite column reaches the high value, it also can be observed from Fig. (3) that, as D/t value increases the experimental ultimate load decreases.

Figure 6: Failure shape of the specimens after testing

4.2. Effect of the strength of the concrete

It can be observed From Fig.(7) that, the load carrying capacity of the tubes filled with concrete increases as compressive strength of concrete increases, this is attributed to the fact that , the strength of a column depend on the strength of its part which have large fraction of its cross section area (concrete).

Fig.(8) shows a load – axial deformation relationships of the hollow columns and columns filled with concrete having different compressive strength. From this table it can be observed that the stiffness of the columns increases as the compressive strength of concrete filled it increases. This is because the modulus of elasticity of concrete increases as a compressive strength increases. It has been observed that, the ductility of the composite columns improves as compared to the hollow columns (SHS5) as illustrated in Fig(8).

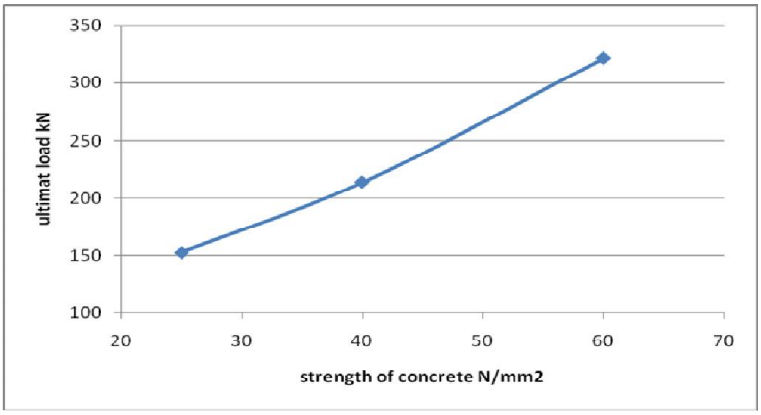

Figure 7: Relationship between ultimate strength and strength of concrete

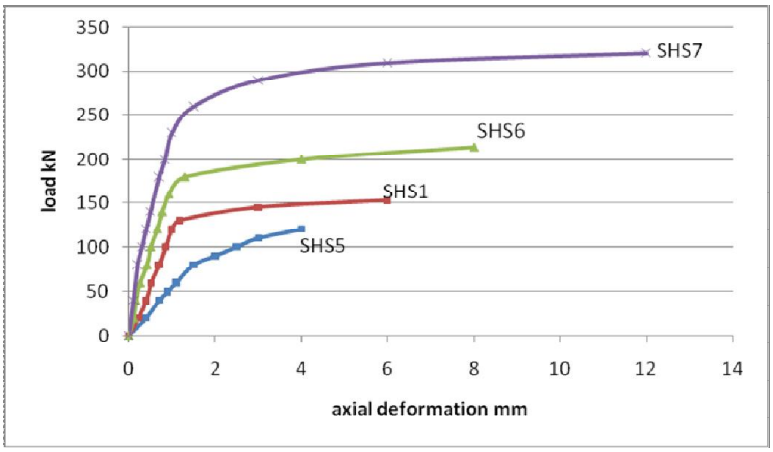

Figure 8: Load versus axial deformation curves for series S2

After failure of SHS4 specimen, it was cut in level of the local buckling zone of tube wall as illustrated in Fig.(9) . This figure reveals the condition of the concrete core and the tube wall at the end of test for SHS4 specimen. It is observed that, there were few voids between the concrete and tube wall in level of the locally buckled region, although diagonal cracks were noted in the concrete core.

In the hollow sections column (SHS5), the failure mode showed that, the wall of tube buckled inward as shown in Fig.(10),but for the columns filled with concrete, its tube walls buckled outward as shown in Fig.(9).

Figure 9: Concrete core after sever local buckling specimen SHS4

Figure 10: Failure mode of series S2

4.3. Effect of slenderness ratio (L/D)

The result of S3 and R2 groups presented in Table (4) showed the effect of L/D ratio on the carrying capacity of hollow and filled aluminum columns, it has been found that the ultimate load of the types of columns decreases with increasing L/D ratio, and this effect is clearer in square sections than it is rectangular section as seen in Fig.(11).

It can be noted from Fig.(11) that, after L/D ratio of 7, there is no significant effect for the increase of L/D on the ultimate load of hollow and filled columns. This may be due to the fact that, after this L/D ratio the mode of failure directs to lateral buckling failure in column RHS10 and RHS 11 as shown in Fig(12).

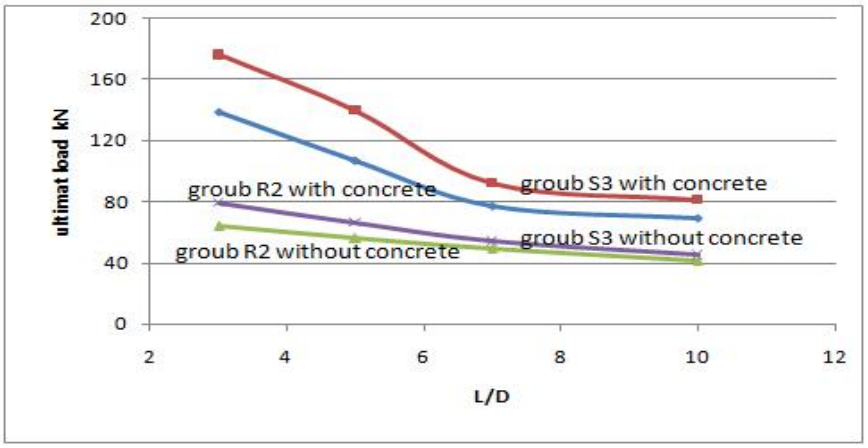

Figure 11: Effect of L/D ratio on ultimate load of groups S3 and R2 specimens

The ultimate load and final failure mode were affected by the strength of the concrete and variation in the L/D ratio of the concrete-filled aluminum column. Specimen SHS9 failed at an ultimate axial load 107 KN. The failure occurred due to the local buckling of aluminum tube and shear stress of the concrete as illustrated in Fig.(13).

S3 Group

Figure 12: failure mod of S3 and R2 groups specimens.

Figure 13: Failure mode of specimen SHS9

The local buckling of the aluminum tube occurred at the level near to the bottom. Specimen SHS10 failed due to wall local buckling of the aluminum tube at the top end, continued to the third height of the specimen end (the ultimate load 140 kN). The failure of the aluminum-concrete composite column SHS11 due to buckling at the middle height of column at 90% of the ultimate failure load (77 kN). For specimen SHS12 increasing the load up to 80% of the ultimate load, the horizontal displacement started and increased until buckling of a single curvature occurred. However the horizontal displacement approximately approached zero up to load level 80% of the ultimate load.

Load-axial displacement relationships for each specimen of S3 and R2 were plotted as shown in Figs. (14) and (15), respectively. First, a linear response appeared prior to yielding of steel tube. After this stage the specimens started to show nonlinear response. The initial tangent modulus of the specimens showed the similar behavior until yielding or softening stages as a linear response. However, the initial tangent modulus of the specimens of slenderness ratio (L/D) are equal to 7 and 10 showing lower values more than those of the rest of the specimens. Specimen SHS12 showed no enhancement in the ductility or in the strength and it occurred after softening stage with an increase in the lateral deformation.

Figures (16) and (17) reveal load – lateral deformation relationships of the hollow and filled specimens that have different L/D ratios for square and rectangular sections respectively. It is found that, at the same load, the lateral deformation increases with the increase of L/D ratio specially for the specimens failed by lateral buckling.

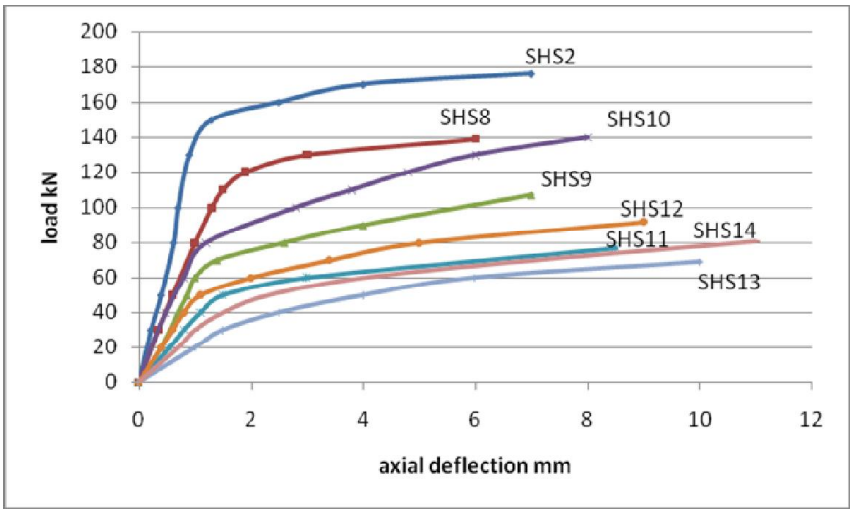

Figure 14: load axial deformation relationship (series S3)

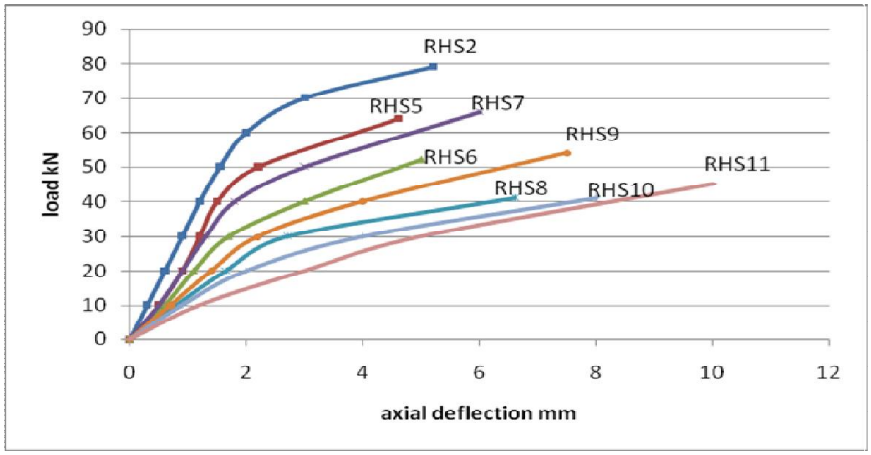

Figure 15: load-lateral deformation relationship (series R2)

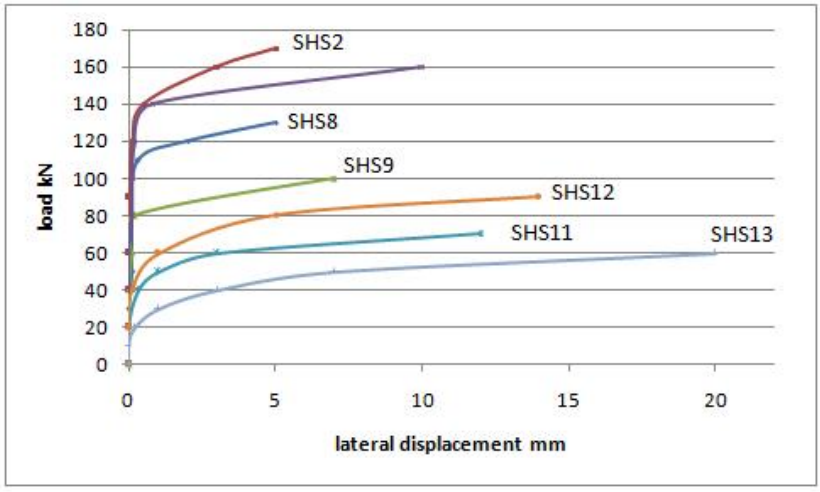

Figure 16: Load lateral deformation relationship (Series R2)

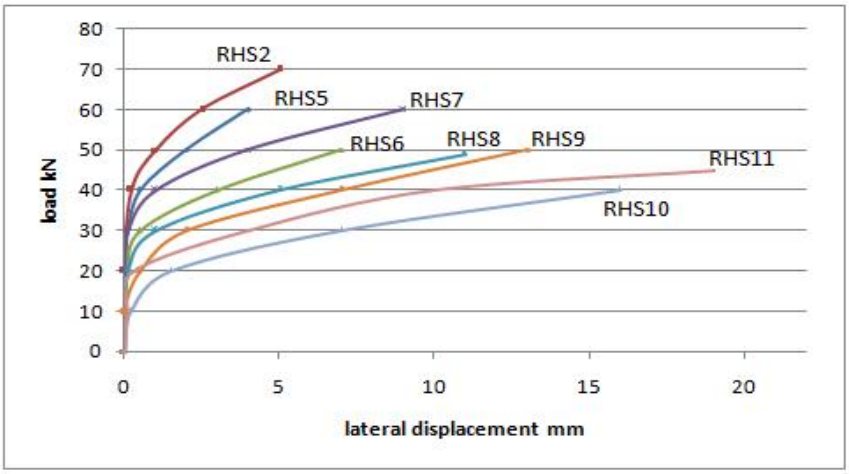

Figure 17: Load lateral deformation relationship (Series S3)

3. Finite element analysis

In parallel with the experimental work, finite element (FE) models were constructed in the ANSYS Version 12.0 program for each of the tested column. Material properties which have been used in experimental work for all columns are adopted in this analysis. For the aluminum material, a bilinear isotropic material model with von Mises yield criterion was used to represent the column nonlinear material behavior. The support and loading conditions of experimental columns were simulated in the analytical model by restraining the appropriate degrees of freedom. The displacement in y direction is equated to zero for all the nodes at the plane of base of the column(uy=0). The aluminum tube was modeled by a SHELL181 element. This element is suitable for analyzing thin to moderately-thick shell structures. It is a four-nodal element with 6 degrees of freedom at each node: translations in the x, y, and z directions, and rotations about the x, y, and z axes. The concrete core of the composite columns was modeled using SOLD 65 element, which has eight nodes with 3 degrees of freedom at each node (translations in the nodal x, y, and z directions) and the material properties were isotropic. This element is capable of plastic deformation, cracking tension (in three orthogonal directions), and crushing in compression. The properties of the concrete and the aluminum entered in the program are similar to that in the experimental program. Contact elements 52 were used to contact the surface of the aluminum sheet to the surface of the concrete. The bond between aluminum and concrete was assumed to be perfect. Fine mesh (25 mm x 25 mm) was provided to simulate the geometry of the analyzed models and to satisfy the requirement of the used element′s aspect ratio. Figure 16 shows a typical full model for one of the analyzed model.

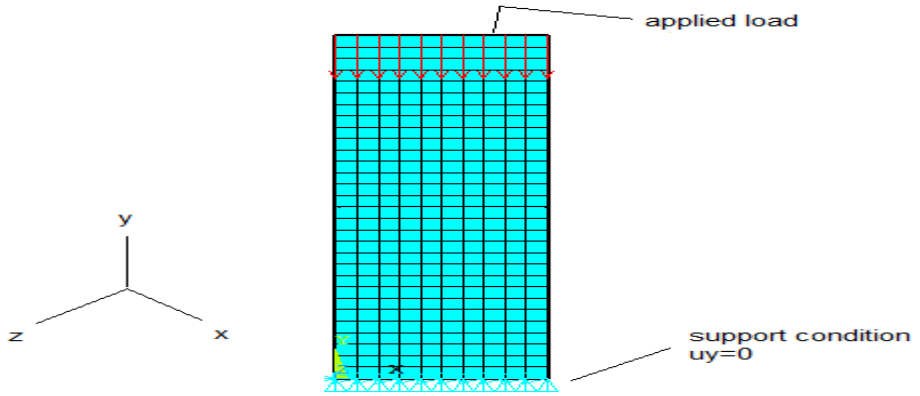

Figure (18): Typical finite element mesh, boundary conditions and applied load.

A summary of experimental and finite element results of columns is presented in Table (5). The predicted ultimate load obtained by ANSYS gives a good agreement with the experimental result. For the most part beams, the finite element ultimate load overestimates than the experimental results by (2%-19%) higher than the experimentally. ANSYS underestimates the strength of the other columns by (2%-11%).Fig.(19) shows the typical specimens after failure and Fig.(20) represents the typical load-deflection plot from the finite element analysis and the experimental results for all columns.

Table (5): Experimental and finite element results of tested columns

Series	Specimens designation	P_{ult} Numerical kN	P_{ult} Experimental kN	P_{ult}Numerical/P_{ult} Experimental
S1	SHS1	149	153	0.97
	SHS2	180	176	1.02
	SHS3	337	343	0.98
	SHS4	460	480	0.95
S2	SHS5	130	121	1.07
	SHS6	220	214	1.02
	SHS7	330	321	1.03
S3	SHS8	125	139	0.89
	SHS9	115	107	1.07
	SHS10	148	140	1.06
	SHS11	70	77	0.91
	SHS12	100	92	1.08
	SHS13	77	69	1.11
	SHS14	95	81	1.17
R1	RHS1	82	70	1.17
	RHS2	87	79	1.10
	RHS3	135	150	0.90
	RHS4	188	200	0.94
R2	RHS5	76	64	1.18
	RHS6	540	562	0.96
	RHS7	75	66	1.13
	RHS8	57	49	1.16
	RHS9	62	54	1.15
	RHS10	49	41	1.19
	RHS11	53	45	1.17

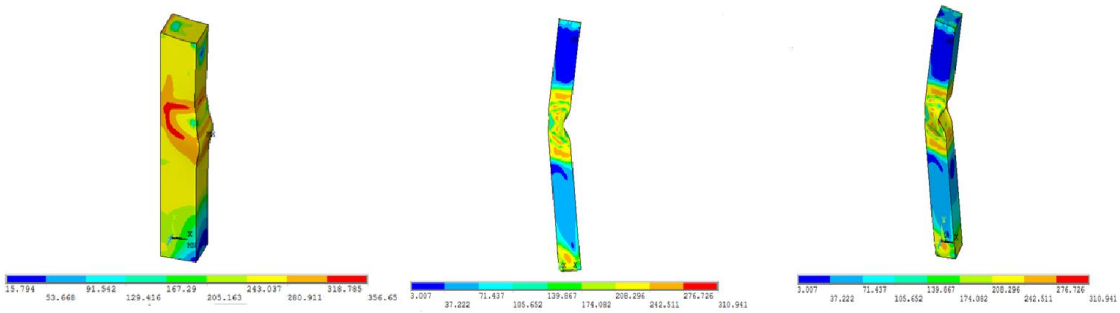

a) Specimen SHS7 b) Specimen SHS9 c) Specimen SHS1

Figure 19: Von-Mises stress distribution for columns

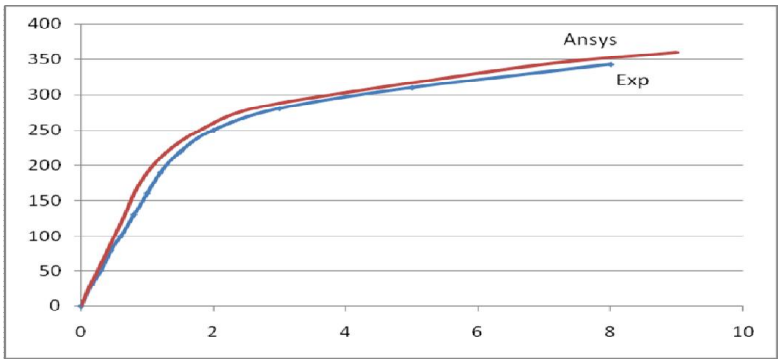

Figure 20: Variation of deflection with load for specimen SHS3

5. Conclusions

This investigation presents the experimental and analytical results of concentrically loaded aluminum tube columns filled with concrete, leads to the following conclusions:

1-The ultimate load of hollow and filled columns increases with the decrease of the depth/ thickness ratio.

2- The compressive strength exhibited very clear effect on overall strength and behavior of the columns filled with concrete.

3- For the length to depth ratios between 3 to7, the strength of columns increases as length to depth ratio increases, but for length to depth ratio more than 7, there is no significant effect on the ultimate load of columns.

4- There is a clear difference between the mode of failure of hollow and filled columns, where in hollow tube section, the buckling of its walls was inward but for filled columns it was outward.

5- The analytical results from modeling in ANASYS program exhibited a good agreement with the experimental results (ultimate load, axial deformations).

Notation

B	Smaller dimension of section
D	Larger dimension of section
L	Length of column
t	wall thickness of aluminum tube
fc’	Compressive strength of concrete

6. References

Aboutaba RS, Machado RI. 1999; Seismic resistance of steel-tubed highstrength reinforced-concrete columns. J Struct Eng ASCE 125(5):485–94.

Australian Standard, 1991;” methods of tensile testing of metals.”, AS 1391, Sydney, Australia, standards association of Australia.

British Research Establishment, 1997, Design of Normal Concrete Mixes, Department of the Environment, second edition, 46pp.

Elremaily A, Azizinamini A. , 2002;Behavior and strength of circular concrete-filled tube columns. J Constr Steel Res;58(12):1567–91.

Feng SZhou and Ben Young , 2009 ;"Concrete-Filled Aluminum Circular Hollow Section Column Tests" Thin-Walled Structures 47 (2009) 1272-1280.

Han LH. 2002; Tests on stub columns of concrete-filled RHS sections. J Constr Steel Res;58(3):353–72.

Liu D, Gho WM. 2005; Axial load behaviour of high-strength rectangular concrete-filled steel tubular stub columns. Thin-Walled Struct 43:1131–42.

Resan S. F. 2014 "Experimental Investigation of Aluminum-Lightweight Concrete Columns". Basrah Journal for Engineering Sciences, Vol.14, No1, 2014.

Sakino K, Nakahara H, Morino S, Nishiyama I., 2004; Behavior of centrally loaded concrete-filled steel-tube short columns. J Struct Eng ASCE 130(2):180–8.

Tao Z, Han LH, Wang DY. 2007; Experimental behaviour of concretefilled stiffened thin-walled steel tubular columns. Thin-Walled Struct 45:517–27.

Uy B., 1998; Local and post-local buckling of concrete filled steel welded box columns. J Constr Steel Res ,74(1–2):47–72.

Uy B. 2001;Static long-term effects in short concrete-filled steel box columns under sustained loading. ACI Struct J ,98(1):96–104.

Uy B. 2001;Strength of short concrete filled high strength steel box columns. J Constr Steel Res 57(2):113–34.

Wang QX, Zhao DZ, Guan P., 2004; Experimental study on the strength and ductility of steel tubular columns filled with steel-reinforced concrete. Eng Struct 26(7):907–15.

Young B, Ellobody E. 2006;Experimental investigation of concrete-filled cold-formed high strength stainless steel tube columns. J Constr Steel Res; 62(5):484–92.

Zhu JH, Young B. 2006;"Test and Design of Aluminum Alloy Compression Members". J Struct Eng ASCE 132 (7); 1096-107.